
Autofluorescence microscopy as a method for the documentation of cephalopod paralarvae and juveniles

Michael METZ, Carolin HAUG, Joachim T. HAUG¹

LMU Munich, Department of Biology II and GeoBio-Center, Großhaderner Str. 2, 82152 Planegg-Martinsried, GERMANY;

¹ Corresponding author: e-mail joachim.haug@palaeo-evo-devo.info

ABSTRACT. In the field of zoological (and palaeontological) research, accurate documentation methods for the exo-morphology are essential. Here we propose a new method for the documentation of cephalopod paralarvae and juveniles. For documenting small-sized cephalopods autofluorescence microscopy offers numerous advantages for the presentation of outer body parts and surface structures in high resolution, partially also of internal structures such as the gladius. Structures are especially well-contrasted compared to other imaging methods, such as white-light microscopy, micro- or macrophotography. This facilitates a detailed view in high resolution at even the smallest cephalopod paralarvae. Autofluorescence imaging, combined with composite imaging, creates sharp, evenly illuminated images. In its higher magnification ranges it can be well compared to low-magnifying scanning electron microscopy (SEM) images, but with the advantage that the drying, mounting and preparation needed for SEM is not necessary for autofluorescence microscopy. In contrast the method enables the direct documentation of specimens inside their storage liquid. This is especially important for the investigation of rare specimens, e.g., for historical material from museum collections, or as a pre-documentation for specimens that will be processed further with an invasive method. By the use of different excitation wavelengths it is furthermore possible to either enhance surface structure details or certain inner body structures. Autofluorescence microscopy is also excellent for the imaging of certain types of small-sized fossil cephalopods, not least as the contrast against the matrix can be significantly improved. All these methods and the associated opportunities for studying cephalopod paralarvae are explored in this study.

Introduction

Cephalopods – squids, cuttlefish, octopus and alike – in their early post-embryonic phase are generally termed paralarvae when being planktonic and meeting certain ecological criteria. The term has been introduced to avoid the general difficulties in differentiating whether these early stages should represent true larvae or not [Young, Harman, 1988].

Paralarvae are usually presented in scientific studies as line drawings [e.g. Young, 1991: figs 3–

5; Tsuchiya *et al.*, 1991: figs 11, 12, 14; Diekmann *et al.*, 2002: figs 8, 11, 15; Barón, 2003: figs 1, 6, 8; Kostak, 2003: figs 1, 2; Boyle, Rodhouse, 2005: figs 10.2, 10.7; Mensch, 2010: figs 1, 2, 20; Franco-Santos, Vidal, 2014: fig. 7]. More rarely microphotography with reflected light illumination has been applied [O’Dor *et al.*, 1982: fig. 1; Salpman, 2012]. Both methods have certain limitations concerning the amount of details observable (and presentable). Drawings always include a certain degree of interpretation, which is both advantageous and disadvantageous. For example, taxonomically important structures can be emphasized with drawings [Coleman, 2006].

Standard type macro- or microphotography is often complicated by a relatively low contrast of possibly important structures. Low contrast and another “classical” problem of photography on specimens in liquid, namely reflections, can be both partly overcome with the application of cross-polarized light [e.g., Haug C. *et al.*, 2011], yet only to a certain degree. Cross-polarized light can also be used for improving the contrast for drawing the specimen when observed through the dissection microscope. Yet, drawings and micro- or macrophotography both depend principally on the same type of optics, hence both experience the same type of limitations concerning the observable degree of detail.

Another “classical” documentation method with a higher degree of observable details is scanning electron microscopy (SEM), which has also been applied to study cephalopod paralarvae [e.g., Arnold, Williams-Arnold, 1980: figs 20, 21; Falcon *et al.*, 2000: fig. 2; Shigeno *et al.*, 2001: figs 1D, 3]. The disadvantage of SEM is the necessity for intensive preparation including drying. Drying often leads to artifacts, such as collapse of softer structures, even if applying critical point drying or other methods which at least minimize such a collapse [see discussion in Haug J.T. *et al.*, 2011]. Furthermore, the processing of drying, usually combined with coating and mounting, should not be applied to historical museum specimens, rare material or specimens which should be processed further (for his-

tology, transmission electron microscopy, etc.). Even the more modern type of environmental scanning electron microscopy (ESEM) does not improve the situation. While in principle undried and uncoated specimens can be documented with this method [e.g., Rakocinski, 2010], specimens stored in liquid still would need to be stabilized (by drying or similarly) to document them outside of their storage liquid.

There are different areas of research that would benefit from an improved documentation method for cephalopod paralarvae. For example, identification keys could be supported by photographic images in addition to line drawings of the paralarvae. An advanced documentation would also be beneficial for digital cataloging of specimens from museum collections. Such an approach would also be useful for tackling biogeographical questions, e.g., concerning the native waters of different species [e.g., Tsuchiya *et al.*, 1991; Lefkaditou *et al.*, 2005].

A new documentation method is also especially interesting for the field of exo-morphology, which is again the base for other disciplines, e.g. functional morphology and, with this, inference of autecology. Especially for not easily directly observable species or life stages, functional morphology is a central source of information [see discussion in Haug C., Haug J.T., 2014].

As another extension of exo-morphology, research on ontogenetic development can be improved by applying new documentation methods for comparing various growth stages. Currently, for cephalopods this is also mainly done by the use of line drawings [e.g., Wakabayashi *et al.*, 2005].

Autofluorescence imaging has been established as a useful and promising documentation method, especially for arthropods [e.g., Michels, 2007; Haug J.T. *et al.*, 2011; Kenning, Harzsch, 2013; Rötzer, Haug J.T., 2015]. This method allows the documentation of specimens due to their intrinsic fluorescence. The result is a high-quality image with even illumination and strong contrast. We explore here the possibilities of applying autofluorescence microscopy for the documentation of cephalopod paralarvae. Subsequently, we discuss advantages and limitations of this method.

Material and methods

Material

Investigated material includes extant cephalopod paralarvae and a small sized fossil cephalopod. Extant cephalopod paralarvae came from the collection of the Zoological Museum of the University of Copenhagen, Denmark. About 20 different paralarvae were inspected, three of which have been documented with this method (collection numbers of the specimens: ZMUC-CEP-303, ZMUC-CEP-307,

ZMUC-CEP-309). Specimens have been collected decades ago on various research cruises and since then been stored in 70% ethanol. A single fossil cephalopod came from the private collection of Udo Resch, Eichstätt, Germany. The specimen is comparably small and most likely represents a juvenile. The specimen originates from the lithographic limestones of the Solnhofen area, southern Germany, and is about 150 million years old (Upper Jurassic).

Documentation methods

All extant specimens were documented directly within their storage liquid. The paralarvae were fixed in different positions by a cover slip and small stainless metal objects (nuts and washers, for providing distance and weight) in small Petri-dishes with a coverslip as bottom. The fossil specimen was documented “as is”, dry without covering [e.g. Haug J.T. *et al.*, 2008; Haug C. *et al.*, 2009; Kerp, Bomfleur, 2011].

The documentation was performed with a Keyence BZ 9000 fluorescence microscope; the optics are inverse, hence objectives are below the object. The microscope was equipped with different objectives of 2x, 4x, 10x, 20x and 40x magnification, resulting in an effective magnification of about 20x, 40x, 100x, 200x, and 400x. Three different excitation wavelengths were applied: 377 nm (ultraviolet/blue, DAPI), 473 nm (blue/green, GFP) and 543 nm (green/orange, TRITC).

We also applied different imaging methods for providing comparative images of one of the specimens which was documented with autofluorescence microscopy. For macro-photography we used a Canon Rebel T3i camera equipped with a macro lens (MP-E 65mm) and a Macro Twin Lite (MT24EX) for illumination. The lens was equipped with a polarization filter. Perpendicular polarization filters were placed on the flashes in order to produce cross-polarized light. This enhances the color contrast and reduces reflections [e.g. Hörnig *et al.*, 2014: fig. 2A]. With this set-up also a stereo pair was recorded for representing the topology of the specimen. These methods have been successfully applied to marine small-sized animals [e.g., Haug C., Haug J.T., 2014].

Dissection microscopes are commonly used for documentation (although, as their name suggests, they are optimized for dissecting, not for documenting). We therefore used an Olympus SZ X7 dissection microscope with a Touptek DCM510 ocular camera for documentation. Illumination was provided by an external cold light source. Also here light was cross-polarized.

Better optics (in the sense of producing less artifacts) can be found in compound microscopes. We used a Zeiss Axioplan compound microscope, also with a Touptek DCM510 ocular camera for

documentation. Two types of illumination were used: dark field illumination and reflected light provided by external LEDs. Also here light was cross-polarized.

To overcome the limited depth of field in all settings, several images were taken along the z-axis as an image stack. To overcome the limited field of view in some of the images several adjacent image details were recorded [composite imaging; Haug J.T. *et al.*, 2008; Haug C. *et al.*, 2009; Kerp, Bomfleur, 2011].

Image processing

Image stacks were fused into a single sharp image with CombineZM or CombineZP. Fused images were stitched to a panorama image with Microsoft Image Composite Editor (ICE), Adobe Photoshop CS3 or CS4 [for more details on this process = composite imaging, see, e.g., Haug J.T. *et al.*, 2011].

For some images the same image detail was recorded under two different exposure times. To combine the resulting panorama images of the two exposure times, the brighter image was placed as a layer above the darker one. The overexposed structures were then selected by the magic wand tool. A strong feather was applied and the overexposed areas were deleted. These resulting images hence show structures of both exposures [e.g. Haug C. *et al.*, 2013]. A similar process was applied to combine images recorded under different wave-lengths.

All images were optimized for levels, brightness, contrast and sharpness in Adobe Photoshop CS3. Dirt particles and fusion artifacts, such as halos, were removed manually with the lasso tool (with a weak feather). To facilitate a better identification of the structures for the reader in some images structures were additionally color-marked.

Results and evaluation of the images

The outer surface of the cephalopod paralarvae investigated here show intense autofluorescence (Figs. 1–3). This allowed the documentation of the cephalopod paralarvae with composite fluorescence microscopy with a high degree of detail. It remains unclear why the specimens show this type of fluorescence. It is possible that this is an original characteristic of the specimens. Yet, it is also possible that the chemicals used for fixation caused or at least enhanced the fluorescence capacities of the specimens. It remains unclear which substances were originally used for fixation, but it seems likely that 3–4% formaldehyde was used for initial fixation.

While the fluorescence capacities of the specimens are excellent, the fluorescence capacities of dust and especially cotton wool lint are significantly higher, at least under short wavelengths (especially

UV). Hence, it is advisable that the ethanol and the paralarvae themselves are kept free of all dirt, at least as dirt free as possible. Especially lint can be a problem during the imaging process. Lastly, not all paralarvae showed similarly good results under the same wavelengths; hence not all specimens were documented with the same settings. For each specimen optimal settings were identified by a simple try-and-error strategy.

Specimen 1

The first specimen was documented under DAPI settings (Fig. 1 A–D) and TRITC settings. Most (but not all) specimens of paralarvae have a strong intrinsic fluorescence at a wavelength of 377 nm (DAPI setting).

DAPI settings reveal various details of the outer surface (Fig. 1 A–D). In contrast, illumination with TRITC gives a slightly semi-transparent impression of the outermost skin. Fine wrinkles which are prominent under DAPI settings (Fig. 1A) are not apparent under TRITC settings (Fig. 1E). It seems that under the latter wavelength light penetrates deeper into the skin so that the underlying structures are shining through. This is especially apparent at the eyes, where more details are apparent under TRITC settings compared to the DAPI setting.

The chromatophores are clearly set off as darker spots under DAPI settings (Fig. 1 A, F), but are hardly visible under TRITC settings (Fig. 1E). Hence, for this specimen DAPI settings were used to document it from all sides (Fig. 1 A–D, G). As the body form is more or less compact, it was relatively easy to place the specimens in the different positions. Due to the good contrast, structures can be spatially separated well from each other, also smaller ones such as the suckers (Fig. 1 G, I compare to 1H). This is also true for the unusual, but important, functionally frontal view. As we used an inverse microscope, the specimen could be placed in a corner of a compartment in the Petri-dish to have it standing “on the mouth”.

Here it also becomes apparent that there are some fusion artifacts around the arms, due to the high depth of the image. For higher magnifications (Fig. 1I) the deeper areas were therefore manually digitally removed. The resolution of details still remains at a high degree. It was even possible to document difficult to access structures, such as the buccal apparatus with the jaws.

Specimen 2

This specimen is a paralarva of a *Chiroteuthis* species. The paralarvae of *Chiroteuthis* can reach quite astonishing sizes of several centimeters. Despite their size, also specimens of this size can well be documented with the aid of autofluorescence

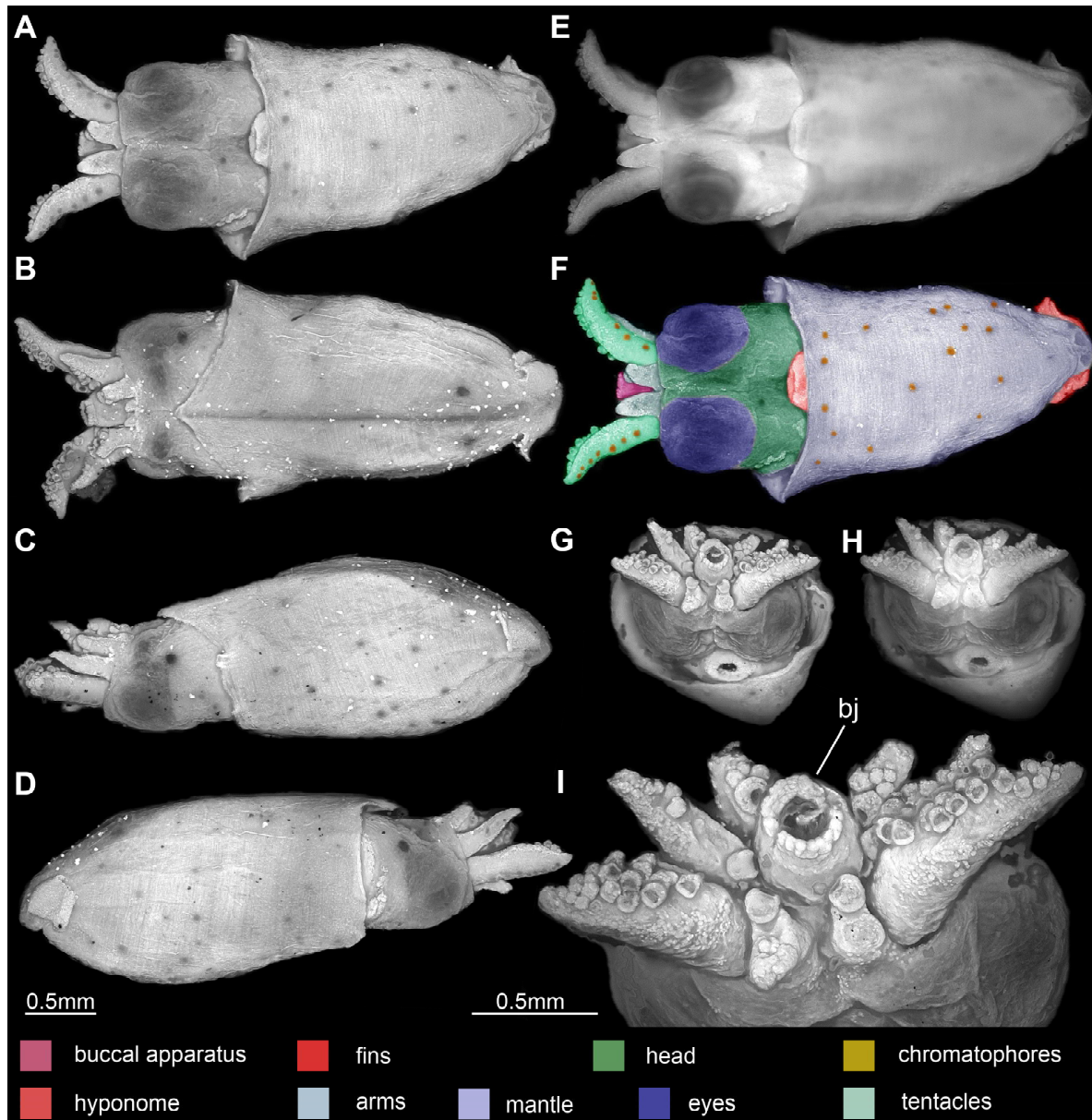


FIG. 1. Paralarva of teuthid cephalopod (total length 2.5 mm) (ZMUC-CEP-307). **A.** Functional ventral view (DAPI). **B.** Functional dorsal view (DAPI). **C.** Lateral view on the left side (DAPI). **D.** Lateral view on the right side (DAPI). **E.** Functional ventral view (TRITC). **F.** Colour-marked version of **A** (colours given in the legend). **G.** Functional frontal view (DAPI). **H.** Functional frontal view (TRITC). **I.** Close up in functional frontal view, with details of tentacles and mouth region (DAPI). Abbreviation: bj = buccal apparatus with jaws.

РИС. 1. Параларва десятирукого головоногого (общая длина 2,5 мм) (ZMUC-CEP-307). **A.** Вид с функционально вентральной стороны (DAPI). **B.** Вид с функционально дорсальной стороны (DAPI). **C.** Вид слева (DAPI). **D.** Вид справа (DAPI). **E.** Вид с функционально вентральной стороны (TRITC). **F.** Раскрашенная версия **A** (обозначения для цветов приведены внизу рисунка). **G.** Фронтальный вид (DAPI). **H.** Фронтальный вид (TRITC). **I.** Увеличенный фрагмент фронтального вида, показывающий детали щупалец и ротового аппарата (DAPI). Сокращения: bj = буккальный аппарат с челюстями.

(Fig. 2). This also demonstrates, that specimens in a size range of a few centimeters, which would be juveniles in most species, can well be handled. Due to the less compact body shape (compared to specimen 1) it was more challenging to position the specimen. Small stainless metal objects (nuts and washers), placed in the Petri-dish, were used to

“direct” the specimens without occluding structures of the specimen. Also this might prove to be a general necessity for larger specimens which have more elongate body structures. We can also demonstrate that despite the size it is also possible to place the specimen in a way that we can access the mouth region.

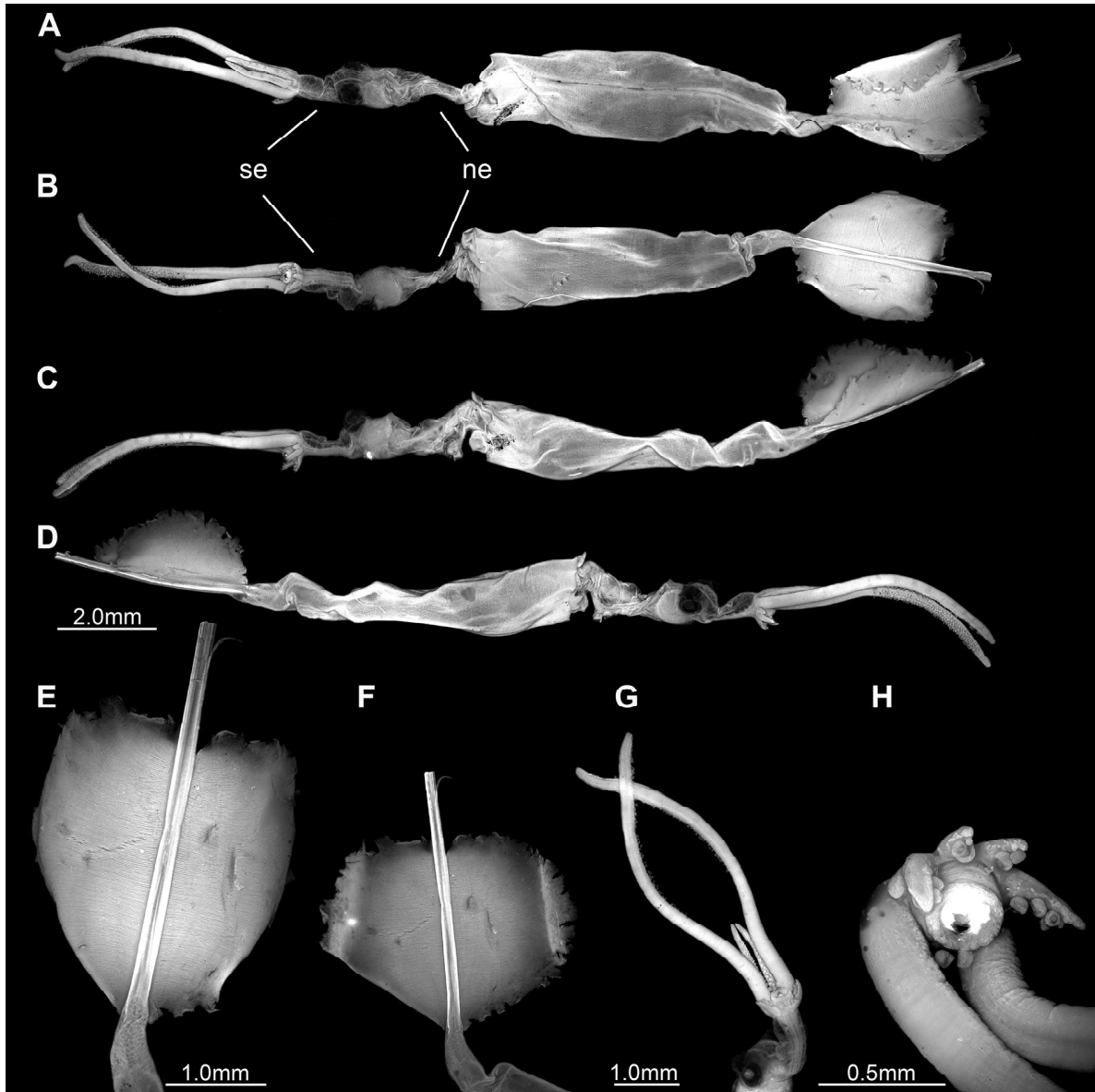


FIG. 2. Paralarva of a species of *Chiroteuthis* (total length 14 mm) (ZMUC-CEP-303). **A.** Functional dorsal view. **B.** Functional ventral view. **C.** Lateral view on the left side. **D.** Lateral view on the right side. **E.** Close-up on the functional posterior region, including fins; note the partly folded fin rims, ventral view. **F.** Same as E, but with unfolded fins. **G.** Close-up on head, functional antero-ventral view. **H.** Functional frontal view on the buccal apparatus. All images under DAPI settings. Abbreviations: ne = neck-like elongation; se = snout-like elongation.

РИС. 2. Параларва *Chiroteuthis* sp. (общая длина 14 мм) (ZMUC-CEP-303). **A.** Вид с функционально дорсальной стороны. **B.** Вид с функционально вентральной стороны. **C.** Вид слева. **D.** Вид справа. **E.** Задний отдел, включая неразвернутые плавники, вентрально. **F.** То же, что E, плавники развернуты. **G.** Увеличенная голова, вид спереди и с вентральной стороны. **H.** Фронтальный вид ротового аппарата. Все изображения с установками DAPI. Сокращения: ne = удлинённая "шея"; se = удлинённая морда.

In case of the *Chiroteuthis* paralarva morphological peculiarities could also be well documented. Among these are the neck-like elongation between mantle and head, and the snout-like elongation between head and the buccal apparatus. Here also DAPI settings proved to be more informative. For example, the texture of the skin located on the dorsal part of the buccal apparatus is well apparent

under these settings (Fig. 2 B, G). It is a reticulated surface structure which is different from the surrounding skin. Also the gladius can be identified inside the (functionally) posterior fin-bearing region (Fig. 2 E, F). The gladius appears to protrude outside the skin. This region also shows the importance of a careful positioning of the specimen. Here in one case, the fins were still folded under them-

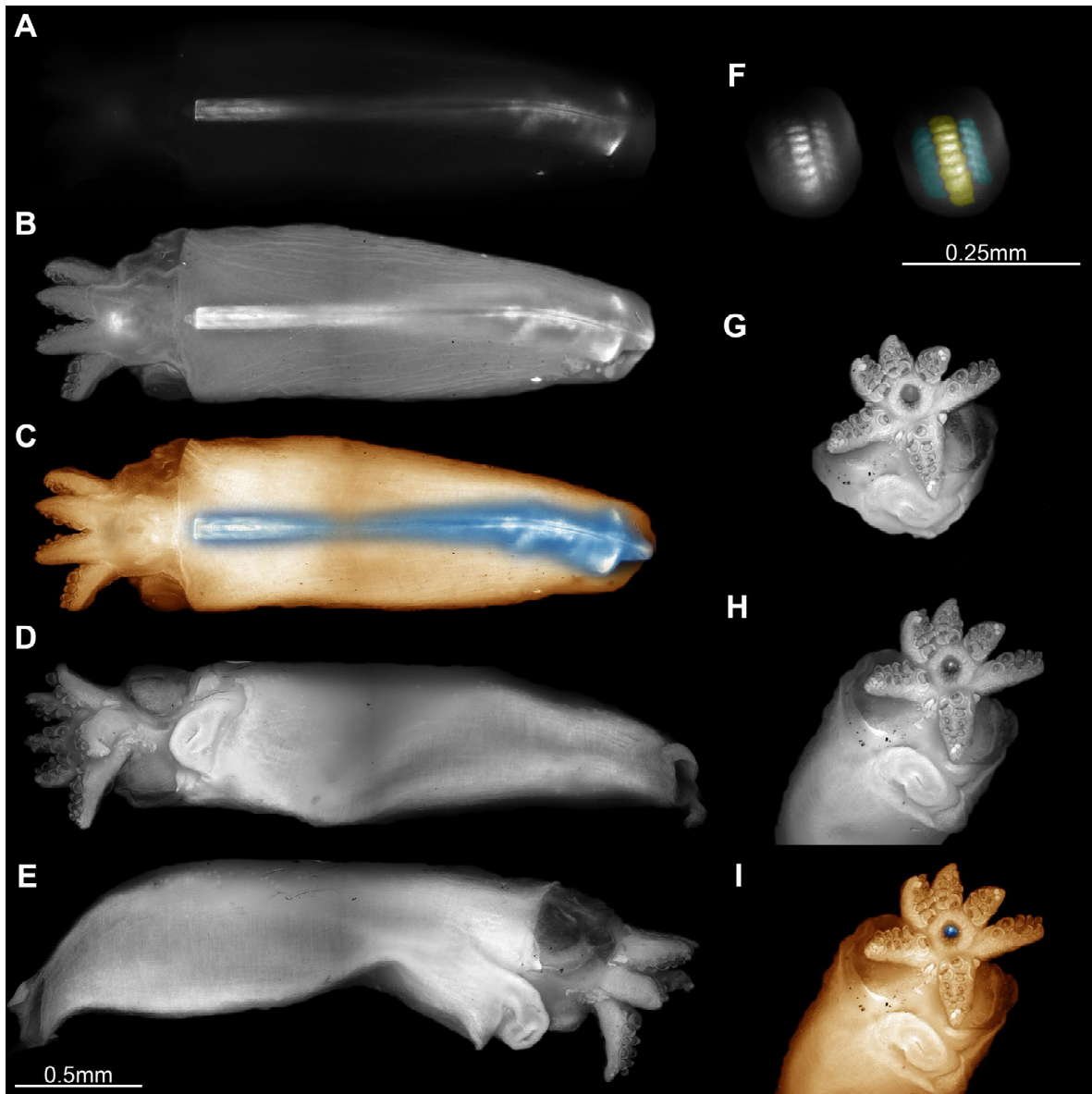


FIG. 3. Image of a decabrachian paralarva at an early stage (total length 2 mm) (ZMUC-CEP-309). **A.** Ventral view with the gladius at lower exposure (DAPI). **B.** Ventral view with the DAPI image of the gladius in lower exposure placed upon a DAPI image of the paralarva in higher exposure. **C.** Colour-marked version of the functional ventral view with the gladius inside the mantle. Orange: GFP image of the paralarva. Blue: DAPI image of the gladius placed upon the GFP image. **D.** Functional ventral view (GFP). **E.** Lateral view of the right side (GFP). **F.** Detail view of the radula inside the mouth at 20x magnification together with a colour-marked version (DAPI). **G.** Functional front view with mouth and arms at 10x magnification (GFP). **H.** Functional front view of the mouth and arms together with the radula inside the mouth (DAPI). **I.** Colour-marked version of the functional front view. Orange: GFP image of the paralarva. Blue: DAPI image of the radula placed upon placed upon the GFP image.

РИС. 3. Параларва Decabrachia на ранней стадии (общая длина 2 мм) (ZMUC-CEP-309). **A.** Вентральный вид с гладиусом, сфотографированный при малой экспозиции (DAPI). **B.** DAPI изображение гладиуса, полученное при малой экспозиции и наложенное на DAPI изображение параларвы, снятое с большей экспозицией (вид с вентральной стороны). **C.** Раскрашенная версия вентрального вида с гладиусом внутри мантии. Оранжевым помечено GFP изображение параларвы; голубым – DAPI изображение гладиуса, помещенное на GFP изображение. **D.** Вид с вентральной стороны (GFP). **E.** Вид справа сбоку (GFP). **F.** Изображение радулы внутри рта при 20x увеличении и раскрашенная версия (DAPI). **G.** Вид спереди со ртом и руками при 10x увеличении (GFP). **H.** Вид спереди рта, рук и радулы внутри рта (DAPI). **I.** Раскрашенное изображение вида спереди. Оранжевым помечено GFP изображение параларвы; синим – DAPI изображение радулы, наложенное на GFP изображение.

selves, providing an incorrect impression of the fins morphology.

Specimen 3

This specimen is more similar to specimen 1,

i.e., it is again more compact than specimen 2. Yet, it shows slightly different fluorescence capacities. When documenting the specimen under DAPI settings, there was an extremely overexposed struc-

ture visible shining through the mantle. After the brightness was turned down, the overexposed structure turned out to be the gladius inside the mantle (Fig. 3A). At these short exposure times it was not possible to observe other structures of the paralarva as these were too dark. Under GFP settings the specimen shows nearly the same details as under DAPI settings (Fig. 3 D, E, G), but without the strong overexposure of the gladius.

We therefore combined the two images to allow a clear correlation of the gladius to the surrounding “soft parts” (Fig. 3C). With these fluorescence capacities it was possible for this specimen to access information of an inner structure, namely the gladius, without preparation of the specimen.

Another structure showing comparable fluorescence capacities to the gladius is the radula (Fig. 3F). Due to the small size of the specimen, and resulting small size of the radula it proved to be difficult to resolve the individual teeth of the radula. The radula is additionally effectively seen through some occluding structures (soft parts) additionally reducing lateral resolution.

This example shows the principle limitations of epifluorescence microscopy. A better spatial resolution might be achieved with a confocal laser scanning microscope (CLSM). Yet, it would need to be an inverse microscope to allow the specimen to be placed in the right orientation. Unfortunately, we had no microscope available on which we could pose the specimen correctly as CLSM microscopes are often optimized for slide mounted objects.

Specimen 4

This specimen is a fossil one. It is larger than the other specimens, but still in the size range of certain paralarvae, e.g., specimen 2. Yet, the fossil most likely does not represent a paralarva, but a juvenile. The specimen preserved relatively hard parts, the gladius, but also numerous soft parts, among others parts of the gut, ink sack and either skin or muscle tissue of the mantle (Fig. 4).

All structures have a good contrast under all wavelengths (Fig. 4 A-C). As for the extant specimens there is the highest degree of small details under DAPI settings, yet there are also the same problems with dust. The best contrast, and no noise of the dust, is achieved by applying GFP settings. The structures appear most even under TRITC settings. Hence, depending on which aspect should be emphasised, one can choose the respective wavelength.

Discussion

Autofluorescence of extant cephalopod paralarvae

The central observation reported here: cephalopod paralarvae show a certain degree of autofluorescence and can hence be documented with auto-

fluorescence microscopy. This observation is not trivial. Autofluorescence (on extant specimens) has so far been mainly used for documenting arthropods [e.g. Michels, 2007; Haug J.T. *et al.*, 2011; Kenning, Harzsch, 2013; Rötzer, Haug J.T., 2015]. Also some examples have been given for other invertebrates, e.g., echinoderms [Haug J.T. *et al.*, 2011]. For molluscs so far mainly specific structures have been documented using autofluorescence, for example the radula [Haug J.T. *et al.*, 2011].

We cannot be sure whether the fluorescence capacities are an intrinsic characteristic of the specimens or were influenced by the fixation process. Yet, we can state that autofluorescence documentation is possible for museum specimens. Whether the method is applicable for freshly killed material or even live specimens is currently unclear and demands further experiments.

Autofluorescence in fossil specimens

The fossil included for comparison here came from the lithographic limestones of southern Germany. The fossil is most likely preserved as calcium phosphate, or (bio-)apatite. This appears to have a good fluorescence capacity compared to the calcium carbonate matrix, which has a weak [but not absent, see e.g. Haug C. *et al.*, 2014] capacity. Autofluorescence in combination with macrophotography has been used for documenting soft parts in fossil cephalopods successfully [e.g. Fuchs *et al.*, 2009]. For small sized specimens only one putative specimen without preserved soft parts, only the gladius, has been documented with autofluorescence microscopy [Haug J.T. *et al.*, 2012]. Here we demonstrate that small sized specimens with soft parts preservation can well be documented with this method.

The advantage of autofluorescence microscopy

So far we have demonstrated that the method is well applicable to specimens of cephalopod paralarvae. Here we partly repeat parts of the discussion on advantages of autofluorescence imaging given by Haug J.T. *et al.* [2011], and focus on the application of that approach to cephalopod paralarvae from museum collections.

1. Highly contrasted images:

The autofluorescence images show an extremely high contrast. This is especially apparent in comparison with more common methods. The lowest contrast is clearly provided by the photograph through the dissection microscope (Fig. 5A), although the images have been optimized as described in the method section. Slightly more details can be seen under the same illumination but better lens systems, either compound microscopy (Fig. 5B) or high-magnification macrophotography (Fig. 5D);

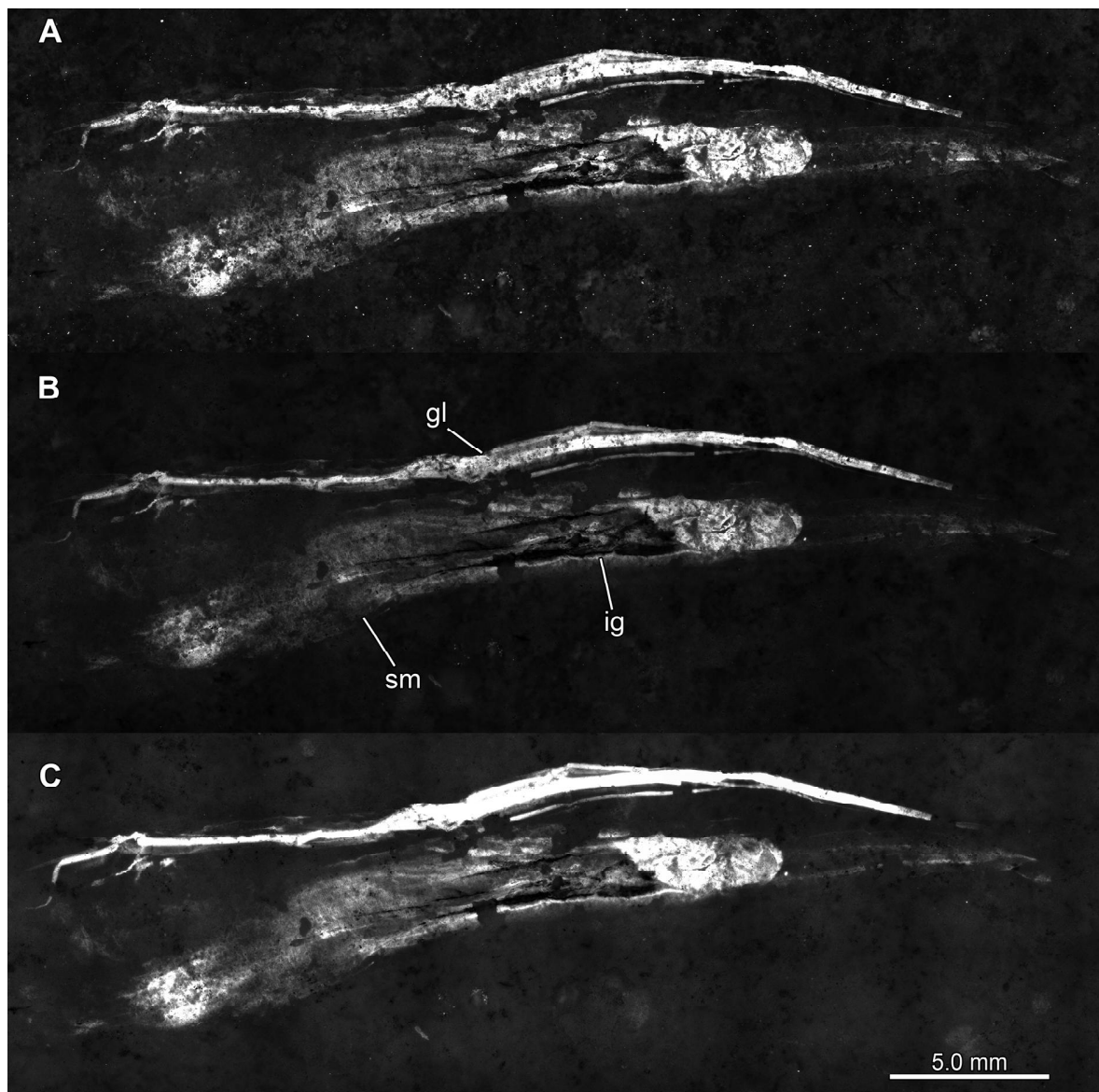


FIG. 4. Image of an unidentified cephalopod fossil (total length 35 mm). The head and the arms have not been preserved. **A.** Image taken with a wavelength of 377 nm (DAPI fluorescence). **B.** Image taken with a wavelength of 473 nm (GFP fluorescence). **C.** Image taken with a wavelength of 543 nm (TRITC fluorescence). Abbreviations: gl = gladius; ig = ink sac or gut; sm = skin or musculature.

РИС. 4. Изображение неопределенного ископаемого головоногого (общая длина 35 мм). Голова и руки не сохранились. **A.** Изображение, полученное при длине волны 377 нм (DAPI флюоресценция). **B.** Изображение, полученное при длине волны 473 нм (GFP флюоресценция). **C.** Изображение, полученное при длине волны 543 нм (TRITC флюоресценция). Сокращения: gl = гладиус; ig = чернильный мешок или кишечник; sm = кожа или мускулатура.

yet most details visible in the autofluorescence image are still not resolvable. The introduction of an additional depth cue, stereo imaging (Fig. 5E) does not further improve this situation.

Slightly more details can be resolved with transmitted light under dark field settings (Fig. 5C). Here the chromatophores can be slightly seen. Also it is possible to recognize the slight striation of the surface. Yet, with this illumination the more central parts are quite dark, as the light hardly can penetrate this thicker region. While resolving some of the

details better than images under reflected light, structures well apparent under the latter can be hardly seen here (e.g. the funnel).

The only method that can show the same details as provided here by autofluorescence imaging is scientific drawing (Fig. 5F). Yet, we have to ask, how have the details shown in the drawing been seen? With the “standard” methods they are difficult to observed. It is possible that such informative drawings were based on freshly killed specimens observed in transmitted light. Freshly killed speci-

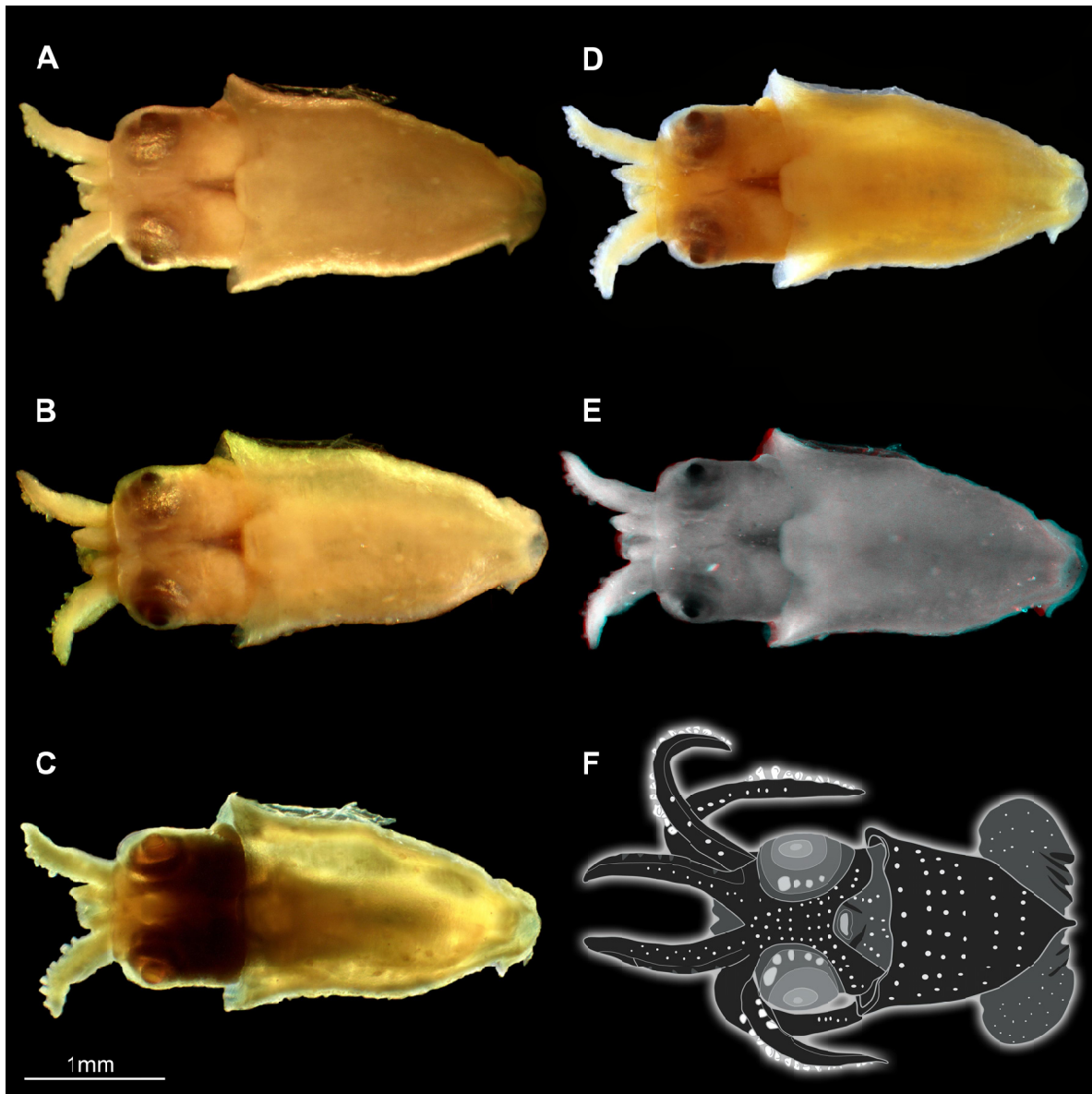


FIG. 5. Comparison of images of a teuthid cephalopod paralarva with different classic imaging methods (ZMUC-CEP-307). It is the same paralarva as in figure 1 (except for the line drawing). **A.** Olympus SZ X7 dissection microscope with reflected light. **B.** Zeiss Axioplan microscope with polarized reflected light. **C.** Zeiss Axioplan microscope with reflected light at darkfield settings. **D.** Macro image taken with a Canon Rebel T3i camera. **E.** Macro-stereo-anaglyph, please use red-cyan glasses to view. **F.** Line drawing; modified after Diekmann *et al.* (2002, fig. 4).

РИС. 5. Сравнение изображений параларвы десятирукого головоногого (та же, что на Рис. 1, за исключением 1F) (ZMUC-CEP-307). **A.** Стереомикроскоп Olympus SZ X7 с падающим светом. **B.** Микроскоп Zeiss Аxioplan с поляризованным падающим светом. **C.** Микроскоп Zeiss Аxioplan с отраженным светом и темным полем. **D.** Макроизображение, полученное камерой Canon Rebel T3i. **E.** Макро стереоизображение (используйте красно-синие очки). **F.** Штриховой рисунок, по Diekmann *et al.* [2002, fig. 4].

mens have likely been more transparent. As a summary we can state that on museum specimens no method facilitates resolution of the same details as autofluorescence imaging.

2. No need for intensive preparation:

While the contrast and degree of details resolvable by autofluorescence imaging is very high, the

necessary preparation is extremely low. Methods with a comparable degree of detail (or higher) such as SEM imaging demand for a complex preparation including drying and coating [e.g., Wanninger, Haszprunar, 2001; Shigeno *et al.*, 2008]. Such preparation methods should not be applied to type material and historical or rare material. Museum material should be handled in a preserving way so that

following generations would also have the possibility to study such material.

Another disadvantage of SEM imaging is the type of mounting. If the specimen is glued on the ventral side onto the SEM stub, only the dorsal side can be studied. With autofluorescence imaging we have been able to access the specimens from all sides.

In cases when the specimens need to be processed further, SEM preparation can not be applied. For example, material which should be used later for histological section or ultra-thin section for TEM studies cannot be pre-documented by SEM. Yet, such material can be perfectly documented with autofluorescence imaging. This will allow to pre-document cephalopod paralarvae before further processing.

3. Widely applicable:

Epi-fluorescence microscopes as used here are comparably widely available. Many institutions have microscopes of this type. Also many microscopes can be subsequently equipped with an additional epifluorescence set-up. It is even possible to use cheap filters (e.g. stereo glasses) to build a simple fluorescence set-up as used for macro-fluorescence. Here it will most likely be necessary to use very strong lamps [or simply more of them; see comparable conditions with set-up for polarised light in Haug J.T. *et al.*, 2013].

Ocular cameras (as used here for some comparative images, Fig. 5) can nowadays also be cheaply purchased. With this situation, autofluorescence imaging indeed has the potential to be widely used, even in field stations or out in the field (here the only problem will be to provide a dark surrounding).

Conclusions and outlook

With all these advantages autofluorescence imaging has the potential to act as a new standard for the documentation of cephalopod paralarvae. It provides highly contrasted images and demands for no special preparation and can be performed with widely available set-ups.

Autofluorescence images of cephalopod paralarvae could be used in the future, not only in the description of exomorphology, but also for:

- Amending identification keys with autofluorescence images for facilitating better identification; thus improving teaching of biodiversity courses and scientific studies of, e.g. morphology, developmental biology or biogeography.

- Cataloging and making museum collections easier publicly available, here series of autofluorescence images acting as a type of virtual specimens.

Acknowledgements

We thank Tom Schiøtte and Martin Vinther Sørensen, both Zoological Museum of the University of Copenhagen (ZMUC), for providing access to specimens of the collections of the ZMUC. Udo Resch, Eichstätt, is thanked for the loan of the fossil specimen from his private collection. We are very grateful to Gideon T. Haug, Neuried, for producing the line drawing in Fig. 5F. CH is currently kindly supported by a Bavarian Equal Opportunities Sponsorship (BGF) of the LMU Munich. JTH is grateful for being funded by the German Research Foundation (DFG Ha 6300/3-1). This project was made possible with funds of the Lehre@LMU initiative of the LMU. All authors would like to thank J. Matthias Starck, LMU Munich, for his support. Finally, we thank all people involved in programming open access or shareware software, such as CombineZM/ZP, Gimp and OpenOffice.

References

- Arnold M.J., Williams-Arnold L.D. 1980. Development of the ciliature pattern on the embryo of the squid *Loligo pealei*: a scanning electron microscopy study. *Biological Bulletin*, 159: 102-116.
- Barón P.J. 2003. The paralarvae of two South American sympatric squid: *Loligo gahi* and *Loligo sanpaulensis*. *Journal of Plankton Research*, 25: 1347-1358.
- Boyle P., Rodhouse P. 2005. *Cephalopods: ecology and fisheries*. Blackwell Publishing, Oxford: 161-175.
- Coleman C.O. 2006. Substituting time-consuming pencil drawings in arthropod taxonomy using stacks of digital photographs. *Zootaxa*, 1360: 61-68.
- Diekmann R., Piatkowski U., Schneider M. 2002. Early life and juvenile cephalopods around seamounts of the subtropical eastern North Atlantic: illustrations and a key for their identification. *Berichte aus dem Institut für Meereskunde an der Christian-Albrechts-Universität, Kiel*, 326: 1-42.
- Falcon L.I., Vecchione M., Roper C.F.E. 2000. Paralarval gonatid squids (Cephalopoda: Oegopsida) from the Mid-North Atlantic Ocean. *Proceedings of the Biological Society of Washington*, 113(2): 532-541.
- Franco-Santos R.M., Vidal E.A.G. 2014. Beak development of early squid paralarvae (Cephalopoda: Teuthoidea) may reflect an adaptation to a specialized feeding mode. *Hydrobiologia*, 725: 85-103.
- Fuchs D., Bracchi G., Weis R. 2009. New octopods (Cephalopoda: Coleoidea) from the late Cretaceous (Upper Cenomanian) of Hakel and Hadjoula, Lebanon. *Palaeontology*, 52: 65-81.
- Haug C., Haug J.T. 2014. Defensive enrolment in mantis shrimp larvae (Malacostraca: Stomatopoda). *Contributions to Zoology*, 83: 185-194.
- Haug C., Haug J.T., Waloszek D., Maas A., Frattigiani R., Liebau S. 2009. New methods to document fossils from lithographic limestones of southern Germany and Lebanon. *Palaeontologia Electronica*, 12(3): 6T; 12 pp.
- Haug C., Mayer G., Kutschera V., Waloszek D., Maas A., Haug J.T. 2011. Imaging and documenting gammarideans. *International Journal of Zoology*, Article ID 380829, doi:10.1155/2011/380829

- Haug C., Shannon K.R., Nyborg T., Vega F.J. 2013. Isolated mantis shrimp dactyli from the Pliocene of North Carolina and their bearing on the history of Stomatopoda. *Bolétin de la Sociedad Geológica Mexicana*, 65: 273-284.
- Haug C., Briggs D.E.G., Mikulic D.G., Kluessendorf J., Haug J.T. 2014. The implications of a Silurian and other thylacocephalan crustaceans for the functional morphology and systematic affinities of the group. *BMC Evolutionary Biology*, 14: art. 159.
- Haug J.T., Haug C., Ehrlich M. 2008. First fossil stomatopod larva (Arthropoda: Crustacea) and a new way of documenting Solnhofen fossils (Upper Jurassic, Southern Germany). *Palaeodiversity*, 1: 103-109.
- Haug J.T., Haug C., Kutschera V., Mayer G., Maas A., Liebau S., Castellani C., Wolfram U., Clarkson E.N.K., Waloszek D. 2011. Autofluorescence imaging, an excellent tool for comparative morphology. *Journal of Microscopy*, 244: 259-272.
- Haug J.T., Kruta I., Haug C. 2012. A possible fossil paralarva (Cephalopoda: Coleoidea) from the Solnhofen Lithographic Limestones (Upper Jurassic, southern Germany). *Palaeontologia Electronica*, 15: art. 15.3.28A.
- Haug J.T., Müller C.H.G., Sombke A. 2013. A centipede nymph in Baltic amber and a new approach to document amber fossils. *Organisms Diversity & Evolution*, 13: 425-432.
- Hörnig M.K., Haug C., Herd K.J., Haug J.T. 2014. New insights into dictyopteran early development: smallest Palaeozoic roachoid nymph found so far. *Palaeodiversity*, 7: 159-165.
- Kenning M., Harzsch S. 2013. Brain anatomy of the marine isopod *Saduria entomon* Linnaeus, 1758 (Valvifera, Isopoda) with special emphasis on the olfactory pathway. *Frontiers in Neuroanatomy*, 7: art. 32.
- Kerp H., Bomfleur B. 2011. Photography of plant fossils – new techniques, old tricks. *Review of Palaeobotany and Palynology*, 166: 117-151.
- Kostak M. 2003. Eoteuthoidae – a new family of Late Cretaceous dibranchiate cephalopods (Coleoidea, Decapoda, Teuthina?). *Bulletin of Geosciences*, 78: 157-160.
- Lefkaditou E., Siapatis A., Somarakis S. 2005. Juvenile planktonic cephalopods sampled off the coasts of Central Greece (Eastern Mediterranean) during winter. *Phuket Marine Biological Centre Research Bulletin*, 66: 259-265.
- Mensch R. 2010. A systematic review of the squid genus *Chiroteuthis* (Mollusca: Cephalopoda) in New Zealand waters. *Thesis, School of Applied Science, Auckland University of Technology, New Zealand*.
- Michels J. 2007. Confocal laser scanning microscopy: using cuticular autofluorescence for high resolution morphological imaging in small crustaceans. *Journal of Microscopy*, 227: 1-7.
- O'Dor R.K., Balch N., Foy E.A., Hirtle R.W.M., Johnston D.A., Amaratunga T. 1982. Embryonic development of the squid, *Illex illecebrosus*, and effect of temperature on development rates. *Journal of Northwest Atlantic Fishery Science*, 3: 41-45.
- Rakocinski M. 2010. Sclerobionts on upper Famennian cephalopods from the Holy Cross Mountains, Poland. *Palaeobiodiversity and Palaeoenvironments*, 91: 63-73.
- Rötzer M.A.I.N., Haug J.T. 2015. Larval development of the European lobster and how small heterochronic shifts lead to a more pronounced metamorphosis. *International Journal of Zoology*: art. 345172.
- Salpman A. 2012. Two new records of paralarva in the Eastern Mediterranean (Cephalopoda: Mollusca). *Journal of the Black Sea/Mediterranean Environment*, 18: 197-207.
- Shigeno S., Kidokoro H., Goto T., Tsuchiya K., Segawa S. 2001. Early ontogeny of the Japanese common squid *Todarodes pacificus* (Cephalopoda, Ommastrephidae) with special reference to its characteristic morphology and ecological significance. *Zoological Science*, 18(7): 1011-1026.
- Shigeno S., Sasaki T., Moritaki T., Kasugai T., Vecchione M., Agata K. 2008. Evolution of the cephalopod head complex by assembly of multiple molluscan body parts: evidence from *Nautilus* embryonic development. *Journal of Morphology*, 269: 1-17.
- Tsuchiya K., Nagasawa T., Kasahara S. 1991. Cephalopod paralarvae (excluding Ommastrephidae) collected from western Japan Sea and northern sector of the East China Sea during 1987-1988: Preliminary classification and distribution. *Bulletin of the Japan Sea National Fisheries Research Institute*, 41: 43-71.
- Wakabayashi T., Tsuchiya K., Segawa S. 2005. Morphological changes with growth in the paralarvae of the diamondback squid *Thysanoteuthis rhombus* (Troschel, 1857). *Phuket Marine Biological Centre Research Bulletin*, 66: 167-174.
- Wanninger A., Haszprunar G. 2001. The expression of an engrailed protein during embryonic shell formation of the tusk-shell, *Antalis entalis* (Mollusca, Scaphopoda). *Evolution & Development*, 3: 312-321.
- Young R.E. 1991. Chiroteuthid and related paralarvae from Hawaiian waters. *Bulletin of Marine Science*, 49: 162-185.
- Young R.E., Harman R.F. 1988. "Larva", "paralarva" and "subadult" in cephalopod terminology. *Malacologia*, 29: 201-207.

Автофлуоресцентная микроскопия как метод документирования параларв и ювенильных особей головоногих моллюсков

М. МЕТЦ, К. ХАУГ, И. Т. ХАУГ¹

LMU Munich, Department of Biology II and GeoBio-Center, Großhaderner Str. 2, 82152 Planegg-Martinsried, GERMANY; ¹ автор-корреспондент: e-mail joachim.haug@palaeo-evo-devo.info

РЕЗЮМЕ. Точные методы документации внешней морфологии очень важны в зоологических и палеонтологических исследованиях. Мы предлагаем новый метод документирования параларв и ювениль-

ных особей головоногих моллюсков. Автофлуоресцентная микроскопия имеет многочисленные преимущества при получении изображений внешней морфологии и поверхностных структур с высоким разрешением, частично также и внутренних структур, таких как гладиус. Структуры получаются высоко контрастными, что особенно заметно при сравнении с другими методами получения изображений – световой микроскопии с белым светом, микро- или макрофотографии. Новый метод облегчает получение детальных изображений даже самых маленьких параларв. Автофлуоресцентная фотография, в сочетании с получением композитных изображе-

ний дает резкие равномерно освещенные изображения. При самых больших увеличениях она может сравниться с изображениями, полученными с помощью сканирующего электронного микроскопа с тем преимуществом, что для получения автофлуоресцентной фотографии не надо высушивать и монтировать объекты. Метод позволяет прямое документирование объектов, находящихся в консервирующей жидкости. Это особенно важно для редких экземпляров, например исторического материала в музейных коллекциях. Метод также пригоден для изображения некоторых типов мелких ископаемых остатков головоногих.

